

Quantum Synchronization Blockade: Energy Quantization Hinders Synchronization of Identical Oscillators

Niels Lörch,¹ Simon E. Nigg,¹ Andreas Nunnenkamp,² Rakesh P. Tiwari,^{1,3} and Christoph Bruder¹

¹*Department of Physics, University of Basel, Klingelbergstrasse 82, CH-4056 Basel, Switzerland*

²*Cavendish Laboratory, University of Cambridge, Cambridge CB3 0HE, United Kingdom*

³*Department of Physics, McGill University, 3600 rue University, Montreal, Quebec H3A 2T8, Canada*

(Received 14 March 2017; published 15 June 2017)

Classically, the tendency towards spontaneous synchronization is strongest if the natural frequencies of the self-oscillators are as close as possible. We show that this wisdom fails in the deep quantum regime, where the uncertainty of amplitude narrows down to the level of single quanta. Under these circumstances identical self-oscillators cannot synchronize and detuning their frequencies can actually help synchronization. The effect can be understood in a simple picture: Interaction requires an exchange of energy. In the quantum regime, the possible quanta of energy are discrete. If the extractable energy of one oscillator does not exactly match the amount the second oscillator may absorb, interaction, and thereby synchronization, is blocked. We demonstrate this effect, which we coin quantum synchronization blockade, in the minimal example of two Kerr-type self-oscillators and predict consequences for small oscillator networks, where synchronization between blocked oscillators can be mediated via a detuned oscillator. We also propose concrete implementations with superconducting circuits and trapped ions. This paves the way for investigations of new quantum synchronization phenomena in oscillator networks both theoretically and experimentally.

DOI: [10.1103/PhysRevLett.118.243602](https://doi.org/10.1103/PhysRevLett.118.243602)

Coupled self-oscillating systems can spontaneously synchronize, i.e., align their phase and frequency. This phenomenon [1,2] is observed in a multitude of systems, ranging from the spontaneous blinking of fireflies in unison to the firing of neurons in the human brain and technical applications such as lasers.

The laser is a well-known example of a quantum system that is described as a self-oscillator. However, its steady state far above threshold settles into a coherent state, which is essentially classical [3,4]. Therefore, its synchronization behavior could be fully described within a semiclassical picture so far [5,6], which allows for efficient simulations. Along this line, powerful methods capable of describing large quantum oscillator arrays have been developed, such as complex lasing media [7,8], arrays of optomechanical systems [9,10], and polariton condensates [11–14].

The rapid experimental progress [15–18] in the control of quantum oscillators and in the engineering of their dissipative reservoirs [19–25] is opening the opportunity to study synchronization deep in the quantum regime, where only a few energy states are populated [26–37]. In this regime, semiclassical methods can fail [27], and anharmonicity on the level of single quanta has been identified [34] as a crucial ingredient to demonstrate quantum effects in synchronization.

In this Letter, we discuss a new class of effects in the synchronization of quantum self-oscillators: For the simplest case of two coupled self-oscillators, we find that a finite frequency detuning between different oscillators may enable synchronization in the quantum regime, while synchronization between (nearly) identical self-oscillators

is suppressed. Relatedly, two identical oscillators of different amplitude are found to synchronize better than oscillators of the same amplitude. These findings are in stark contrast to our classical expectation and elude any semiclassical model. The effect generalizes to oscillator networks: identical oscillators, while unable to synchronize directly, can synchronize via a third, detuned, oscillator. We propose possible implementations in a network of superconducting circuits [16,17,38] or using trapped ions [15,39] to demonstrate the effect experimentally. Our Letter opens up a novel regime of synchronization with genuine quantum features that can be observed with state-of-the-art quantum hardware.

Quantum model of the system.—We consider a network of anharmonic oscillators, each described by the Hamiltonian

$$H = \omega a^\dagger a - K(a^\dagger)^2 a^2, \quad (1)$$

where a is a bosonic annihilation operator, ω is the natural frequency of the oscillator, and the Kerr parameter K quantifies the anharmonicity. Crucially, the quantum oscillators are subject to dissipation which drives them into self-sustained oscillations (limit cycles). In the framework of open quantum systems, this is modeled with a Lindblad operator $\mathcal{L} = \mathcal{L}^{(-)} + \mathcal{L}^{(+)}$ consisting of damping $\mathcal{L}^{(-)}$ and amplification $\mathcal{L}^{(+)}$.

To unravel quantum signatures most clearly, we aim for a narrow distribution of Fock states in steady state, ideally a single Fock state. One way to achieve this [40] is with highly nonlinear dissipators

$$\begin{aligned}\mathcal{L}^+ &= \frac{\gamma_+}{2} \sum_n f_+(n) \mathcal{D}[\sqrt{n}|n\rangle\langle n-1|], \\ \mathcal{L}^- &= \frac{\gamma_-}{2} \sum_n f_-(n) \mathcal{D}[\sqrt{n}|n-1\rangle\langle n|],\end{aligned}\quad (2)$$

where the individual terms induce transitions from Fock state $|n\rangle$ to Fock state $|n-1\rangle$. The transition rates $\propto f_+$ (f_-) are highly peaked just below (above) the desired Fock state [41], as illustrated in Fig. 1(a). Our physical implementation described below results in

$$f_{\pm}(n) = \frac{\sigma_{\pm}^2}{(n - n_{\pm})^2 + \sigma_{\pm}^2}, \quad (3)$$

where n_{\pm} and σ_{\pm} are the mean and variance of the Lorentzian. Choosing n_+ near an integer n_0 and n_- near $n_0 + 1$ stabilizes that particular Fock state $|n_0\rangle$, where a high fidelity is achieved if both σ_- , $\sigma_+ \ll 1$. For simplicity, we choose from here on $\sigma_{\pm} = \sigma$, $\gamma_{\pm} = \gamma$, and $n_- = n_+ + 1$.

This corresponds to the extreme quantum limit of self-oscillations, where the energy distribution is so sharp that only a single Fock state is populated. Therefore, due to the phase-number uncertainty, the phase must be in a superposition of all phases. In comparison, the state of an ordinary laser, as described by an incoherent mixture of coherent states, also has an undefined phase of classical uncertainty but not as a result of superposition.

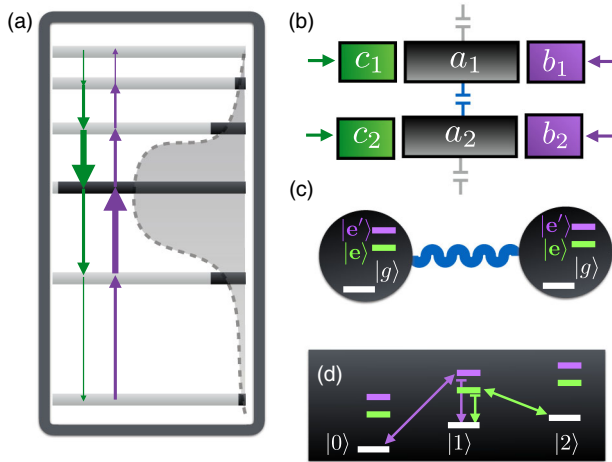


FIG. 1. (a) Illustration of an anharmonic oscillator level structure (grey) with nonlinear amplification (purple) and damping (green) tuned such that a particular Fock state (here, the state $|2\rangle$) is stabilized. The relative thickness of the arrows indicates the transition rate; steady-state population probabilities are depicted in black. The corresponding classical system would have a continuous energy distribution, which is sketched in grey. (b) Implementation with an array of superconducting anharmonic oscillators driven by an amplification cavity (purple) and a damping cavity (green), see main text. (c) Implementation with trapped ions with excited states transition between ground state $|g\rangle$ and excited states $|e\rangle$, $|e'\rangle$ enabling, respectively, sideband cooling and sideband amplification of motion as depicted in (d).

The quantum master equation for the density matrix ρ of a complete network of such self-oscillators (numbered with index j) that are reactively coupled, is given by

$$\dot{\rho} = -i \left[\sum_j H_j + V, \rho \right] + \sum_j \mathcal{L}_j \rho, \quad V = \sum_{j,k} C_{jk} a_j^\dagger a_k, \quad (4)$$

where the commutator between A and B is denoted as $[A, B]$ and the coupling matrix associated with the interaction V fulfills $C_{jk} = C_{jk}^*$ and $C_{jj} = 0$.

Classical model of the system.—We will now introduce the corresponding classical description to be able to compare the quantum system to its classical limit. The self-oscillators in Eqs. (4) can be described by the Langevin equations

$$\dot{\alpha}_j = - \left(i\Omega_j(\alpha_j)\alpha_j + \frac{\Gamma_j(\alpha_j)}{2} \right) \alpha_j - iC_{jk}\alpha_k + \eta_j, \quad (5)$$

with the classical oscillator amplitudes α_j . Here, $\Omega_j(\alpha) = \omega_j - 2K_j|\alpha|^2$ and $\Gamma_j(\alpha) = \gamma_{j-}f_{j-}(|\alpha|^2) - \gamma_{j-}f_{j+}(|\alpha|^2)$ are the amplitude-dependent frequency and damping rate of the j th oscillator, and C_{jk} is the coupling matrix from Eq. (4). Finally, η_j is a white-noise process with correlator $\langle \eta_k(t)\eta_j(t') \rangle = \delta_{kj}\delta(t-t')\gamma_T n_T$, where n_T is the thermal bath occupation and γ_T is the coupling rate to the bath. For conceptual clarity, here, we adopt the fully classical picture neglecting quantum noise induced by the damping terms $\propto \gamma_+$, γ_- . Our main conclusions are not affected by this choice. A derivation of the semiclassical equations including quantum noise can be found in Ref. [42].

Synchronization measures.—To quantify synchronization between two oscillators, we consider the distribution $P(\phi) = \int_0^{2\pi} d\phi_1 d\phi_2 \delta(\phi_1 - \phi_2 - \phi) p(\phi_1, \phi_2)$ of their relative phase ϕ . For the quantum steady state ρ_{ss} , we define $p(\phi_1, \phi_2) = \langle \phi_1, \phi_2 | \rho_{ss} | \phi_1, \phi_2 \rangle$ with phase states $|\phi\rangle = \frac{1}{\sqrt{2\pi}} \sum_{n=0}^{\infty} e^{in\phi} |n\rangle$ [43]. For the classical case, we define $p(\phi_1, \phi_2)$ as the probability of (α_1, α_2) to have phases (ϕ_1, ϕ_2) in the steady state of Eq. (5). In both cases, we choose the synchronization measure [44,45]

$$S = 2\pi \max_{\phi} [P(\phi)] - 1, \quad (6)$$

i.e., a scaled maximum of the relative phase distribution.

Quantum synchronization blockade.—Now, we consider the self-oscillator depicted in Fig. 1(a) coupled to another such self-oscillator with all identical parameters, except for the natural frequencies which are detuned by $\Delta = \omega_1 - \omega_2$. According to classical intuition, the strongest tendency to synchronize as a function of Δ as measured by (6) is always achieved at $\Delta = 0$, where both oscillators are identical. This picture is confirmed by the numerical solution of Eq. (5), which is presented in Fig. 2(a). It is consistent with analytical results obtained in a study of exciton-polariton condensates [12], corresponding to the zero-temperature limit of Eq. (5).

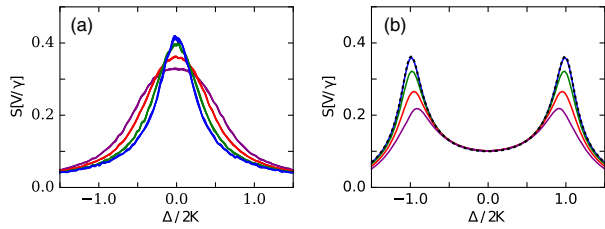


FIG. 2. Synchronization measure S calculated using Eq. (6) as a function of the detuning Δ between two oscillators. All other parameters are identical for both oscillators. Panel (a) shows the result of classical Monte Carlo simulations of Eq. (5), where the width of the line indicates the statistical error. Panel (b) shows results from the numerical steady-state solution of the quantum master equation (4). Classical parameters: $\gamma_T n_t = 0.1\gamma$, $\sigma = 0.2$, $n_+ = 2$, $n_- = 3$, $K = 2\gamma$, $V = 0.1\gamma(\frac{1}{6}, \frac{1}{4}, \frac{3}{8}, \frac{1}{2})$. Quantum parameters: $\sigma = 0.2$, $n_+ = 2$, $n_- = 3$, $K = 10\gamma$, $V = \gamma(0.05, 0.2, 0.35, 0.5)$. In both panels $\gamma_{1\pm} = \gamma_{2\pm} = \gamma$. In first-order perturbation theory (dashed black line), the height of the maximal peak is proportional to the coupling V [46]. Plotting S in units of V for the numerical results, the height of the peak decreases with increasing V , where higher-order effects play a role. The noise level is chosen such that the effect of the thermal noise in panel (a) is approximately as strong as the quantum noise in panel (b).

The classical intuition is not valid in the quantum system described by Eqs. (4). We investigate the same setup with parameters deep in the quantum regime, where the limit cycle is essentially stabilized to a single Fock state $|n_0\rangle$. The numerical result depicted in Fig. 2(b) converges with decreasing coupling strengths to an analytical perturbation theory derived in [46]. The phase synchronization measure is suppressed at $\Delta = 0$, where S has a local minimum. Instead, phase synchronization is now maximal at two peaks at $\Delta = \pm 2K$.

We call this phenomenon the quantum synchronization blockade, as it only occurs deep in the quantum regime, where almost all population is stabilized to a single Fock state. The transition from quantum to classical is visualized in Fig. 3(a): For a narrow Fock distribution around $\sigma = 0.2$, the two maxima of synchronization appear at $\Delta = \pm 2K$, as just discussed. With increasing width σ , the maxima merge to one broad resonance around $\Delta = 0$, as classically expected.

In a second scenario, we consider self-oscillators of identical frequency, now differing only in the amplitude \bar{n} at which they are stabilized. Oscillator 1 is stabilized to an integer $\bar{n} = n_0$ as before, while the amplitude \bar{n} of oscillator 2 is varied continuously. The result is shown in Fig. 3(b): In the quantum regime of small σ , synchronization is maximal at $\bar{n}_2 = \bar{n}_1 \pm 1$; i.e., oscillators with a finite difference in amplitude are most likely to synchronize. Again, the classical intuition, that maximal synchronization will be present for identical oscillators with $\bar{n}_1 = \bar{n}_2$, is confirmed in the classical regime of larger σ .

Thus, in contrast to classical expectation, synchronization of two quantum oscillators can be enhanced by making the oscillators more heterogeneous via detuning their frequency

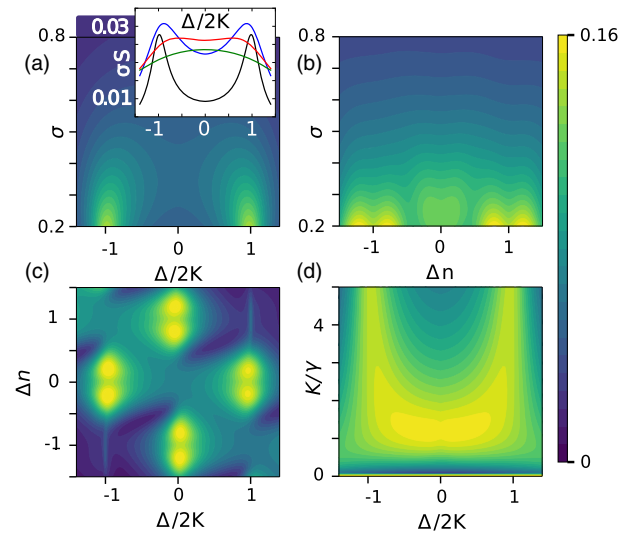


FIG. 3. Plots of synchronization measure S from Eq. 2. (a) Identical oscillators differing only in frequency. Inset shows cuts of S scaled by σ at $\sigma = 0.2, 0.4, 0.6, 0.8$ in black, blue, red, green. (b) Identical oscillators differing only in amplitude. (c) Overview of these resonances in Δn and Δ . (d) Resonances as a function of the Kerr nonlinearity K . Parameters: In the upper panels $n_1^+ \equiv 4$, $n_1^- = n_1^+ + 1$, $V = 0.1\gamma$, $K = \gamma/\sigma_{\pm}$, $\gamma_{1\pm} = \gamma_{2\pm} = \gamma$. In (a), $n_2^+ = 4$, and in (b), $\omega_1 = \omega_2$. In the lower panels, $\sigma_{\pm} = 0.2$, and all other parameters are as above.

or via a mismatch in their amplitude. The result can be explained as follows: For two oscillators to interact efficiently, the process $\propto a_k^\dagger a_j$ of exchanging one excitation must be resonant by conserving energy. For oscillator j in state $|n_j\rangle$ to transfer an excitation to oscillator k initially in state $|n_k\rangle$, it is required that $E(|n_j, n_k\rangle) = E(|n_j - 1, n_k + 1\rangle)$. Writing the energy as $E(|n_j, n_k\rangle) = \langle n_j, n_k | H | n_j, n_k \rangle = \omega_j n_j + \omega_k n_k - K(n_j^2 + n_k^2 - n_j - n_k)$, this leads to the two resonances

$$\Delta + 2K\Delta n \pm 2K = 0, \quad (7)$$

where $\Delta = \omega_j - \omega_k$ and $\Delta n = n_j - n_k$. This resonance condition is one of the main results of our Letter and is illustrated in Fig. 3(c), showing the synchronization measure as a function of both Δ and Δn in the quantum regime. For an illustration of the resonance condition in the case of identical oscillators, see [46].

Equation (7) includes an offset of $2K$ stemming from the mismatch of energy in the exchange of a single quantum of energy described above. Classically, arbitrarily small quanta may be exchanged, so that the offset does not exist. For the oscillators to interact efficiently (and thereby to synchronize), an upward transition of oscillator k must be resonant with a downward transition of oscillator j , or vice versa.

Figure 3(d) shows how the resonances may be resolved for increasing K . For $K = 0$, we have the situation of resonant harmonic oscillators [27], where $P(\phi)$ is a bimodal distribution at $K = 0$. Increasing K first leads to a suppression of

the resonance and, then, to a splitting at $\Delta = \pm 2K$. In this regime, only one maximum of $P(\phi)$ survives.

Oscillator networks.—Having established the quantum synchronization blockade, we now use this understanding to explore consequences for networks of oscillators. In the following, we focus on small networks, as these are easiest to implement experimentally. Consider the three-oscillator network depicted in the inset of Fig. 4(c), where two identical oscillators A and B are coupled indirectly by connecting them with coupling strength V_1 to an oscillator C which has a relative detuning Δ with respect to A and B . First, we look at the case where the direct coupling V_2 between the two identical oscillators is zero. As shown in Fig. 4(a), resonances occur at $\Delta = \pm 2K$ for the synchronization between detuned oscillators, as expected from the two-oscillator case. Figure 4(b) shows that identical oscillators can now synchronize via mediation of the detuned oscillator, again with resonances at $\Delta = \pm 2K$. In this way, the synchronization blockade can be lifted. This finding is also confirmed for the larger network of four oscillators, where two pairs of identical oscillators are connected in a ring in alternating order, see [46].

Conversely, as shown in Figs. 4(c) and 4(d), turning on a coupling V_2 between the identical oscillators can suppress synchronization. This effect is most pronounced for identical oscillators, for which a strip of suppressed synchronization appears along $V_1 \propto V_2$.

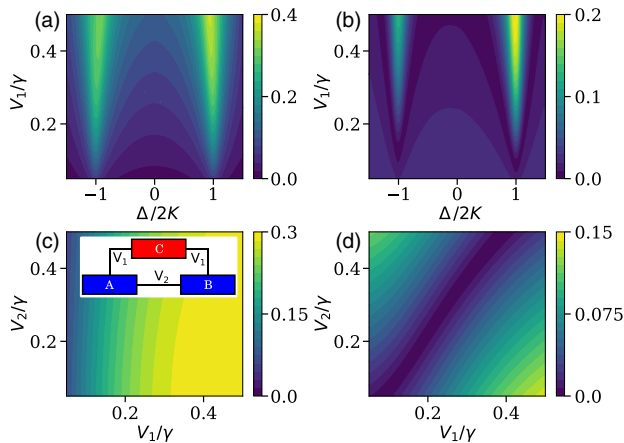


FIG. 4. Synchronization measure S for the network of three oscillators depicted in the inset of panel (c). In the upper panels, two identical oscillators are connected indirectly via an oscillator C with detuning Δ , while the direct link $V_2 = 0$. In the lower panel, the direct link V_2 is also turned on and $\Delta \equiv 2K$. In both panels, $n_1^+ \equiv 1$, $n_j^- = n_j^+ + 1$, $K = 10\gamma$, $\gamma_{1\pm} = \gamma_{2\pm} = \gamma$. In both rows, the left panel shows synchronization between different oscillators and the right panel between identical oscillators. We conclude, from the upper panels (a) and (b), that identical oscillators can be synchronized indirectly via a detuned oscillator. The lower panels indicate that increasing the direct coupling can even decrease synchronization for a strong enough indirect link: In (c) the contour lines bend to the right, while in (d), a strip of suppressed synchronization appears.

Implementation.—Nonlinear damping of the form (3) can be naturally achieved for an anharmonic oscillator mode a coupled to a linear cavity mode c by coupling the number $\propto c^\dagger c$ of the cavity to the quadrature $a + a^\dagger$. Driving the cavity on the red (blue) sideband will lead to a positive (negative) damping [40,42]. Because of the anharmonic level structure, the position of the sidebands depends on the oscillator amplitude. Therefore, in contrast to ordinary sideband cooling, the strength of both damping and amplification nonlinearly depends on the oscillation amplitude.

In a rotating frame of the cavity drive E , the Hamiltonian is given by $H_c = -\delta c^\dagger c + E(c + c^\dagger) + g_0 c^\dagger c(a + a^\dagger)$, where δ is the laser detuning and g_0 is the coupling rate. Defining $g = g_0 \sqrt{\langle c^\dagger c \rangle}$, this can be linearized in the regime of large amplitudes ($\langle c^\dagger c \rangle \gg 1$) as $H_c = -\delta c^\dagger c + g(a^\dagger + a)(c + c^\dagger)$. Assuming that the cavity decay rate κ fulfills $g \ll \kappa$ such that the cavity can be adiabatically eliminated, the parameters of our dissipators (2) are approximately given by [40] $\gamma = 4g^2/\kappa$, $\sigma = \kappa/8K$, and $n_\pm = \pm(\delta_\pm - \omega_0)/2K$.

Thus, to achieve small σ , and thereby stabilize a Fock state, a large anharmonicity to cavity noise ratio $K/\kappa \gtrsim 1$ is required. As depicted in Fig. 3(d) and reflected in the perturbation theory from [46], $K/\gamma \gtrsim 1$ is also necessary. As $\gamma = 4g^2/\kappa$ and $g \ll \kappa$, we have the hierarchy $\kappa > \gamma$, and therefore, only $K/\kappa \gtrsim 1$ remains as the feasibility condition for our specific implementation. This condition is a challenging requirement on the experimental setup. For instance, optomechanical systems, while highly coherent, still lack strong enough anharmonicity. While this may be overcome in the future, e.g., using auxiliary coupling to a Cooper pair transistor [47], we propose an implementation using superconducting circuits and, alternatively, trapped ions. In both platforms, a large anharmonicity $K \gg \kappa, \gamma$ can be achieved with state-of-the-art technology.

An implementation using superconducting circuits is schematically depicted in Fig. 1(b) for the case of two capacitively coupled self-oscillators a_j . To implement larger networks, the array can be extended along the greyed out coupling capacitors. One choice of self-oscillators are transmon qubits [16] which are sufficiently anharmonic while offering a long enough coherence time. The auxiliary cavities for amplification (b_j) and damping (c_j) are coupled to the self-oscillator via an interaction of optomechanical form, $c^\dagger c(a + a^\dagger)$. This can be brought about by embedding a SQUID in the auxiliary cavity [38]. The particular Lorentzian form (3) was assumed as a concrete example, but the scheme is quite general; i.e., any other setup with both nonlinear damping and amplification could be used; any other means of Fock state stabilization such as [23,48,49] will be equally suitable for our purposes.

An implementation using trapped ions is depicted in Fig. 1(c). Ions trapped in adjacent highly anharmonic potentials [39] can become self-oscillators with dissipation engineered as follows: The roles of the cavities for amplification and damping are now played by the internal

level structure of the ion, with one transition driven on the blue sideband and another transition on the red sideband. The use of two transitions is similar to the schemes [27,44] to implement self-oscillators with ions. The ions are naturally coupled via the Coulomb interaction [44,50,51].

We note that, to observe the effect presented here, each node of the network needs to have an anharmonic spectrum consisting of at least three levels, excluding arrays of harmonic oscillators or qubits [46].

Conclusion and outlook.—To conclude, we have described a novel effect referred to as the quantum synchronization blockade, which prevents identical nonlinear oscillators from synchronizing deep in the quantum regime. This is in stark contrast to the classical regime, where oscillators synchronize best when on resonance. Complementarily, we have demonstrated that detuned auxiliary oscillators can lift this blockade by indirectly mediating synchronization between identical oscillators. These effects will be observable in state-of-the-art quantum systems such as superconducting circuits and trapped ions, for which we have proposed concrete implementations. Thus, our Letter opens a new perspective for the exploration of synchronization in Bose-Hubbard–van der Pol-type networks.

We would like to acknowledge helpful discussions with A. H. Safavi-Naeini and S. M. Girvin. This work was financially supported by the Swiss SNF and the NCCR Quantum Science and Technology. A. N. acknowledges support from a University Research Fellowship from the Royal Society and acknowledges support from the Winton Programme for the Physics of Sustainability. All quantum steady-state solutions were obtained in QuTiP [52] and the classical Monte Carlo trajectories were performed in Julia [53]. This work was supported by the European Union’s Horizon 2020 research and innovation programme under grant agreement No 732894 (FET Proactive HOT).

[1] A. Pikovsky, M. Rosenblum, and J. Kurths, *Synchronization: A Universal Concept in Nonlinear Sciences*, Vol. 12 (Cambridge University Press, Cambridge, England, 2003).
 [2] A. Balanov, N. Janson, D. Postnov, and O. Sosnovtseva, *Synchronization: From Simple to Complex* (Springer, New York, 2009).
 [3] C. Gardiner and P. Zoller, *Quantum Noise* (Springer, New York, 2004).
 [4] D. F. Walls and G. J. Milburn, *Quantum Optics* (Springer, New York, 2008).
 [5] W. Schleich and M. O. Scully, *Phys. Rev. A* **37**, 1261 (1988).
 [6] W. Schleich, M. O. Scully, and H. G. von Garssen, *Phys. Rev. A* **37**, 3010 (1988).
 [7] H. E. Türeci, A. D. Stone, and B. Collier, *Phys. Rev. A* **74**, 043822 (2006).
 [8] O. Malik, K. G. Makris, and H. E. Türeci, *Phys. Rev. A* **92**, 063829 (2015).

[9] M. Ludwig and F. Marquardt, *Phys. Rev. Lett.* **111**, 073603 (2013).
 [10] T. Weiss, A. Kronwald, and F. Marquardt, *New J. Phys.* **18**, 013043 (2016).
 [11] P. R. Eastham, *Phys. Rev. B* **78**, 035319 (2008).
 [12] M. Wouters, *Phys. Rev. B* **77**, 121302 (2008).
 [13] S. Khan and H. E. Türeci, *Phys. Rev. A* **94**, 053856 (2016).
 [14] L. M. Sieberer, M. Buchhold, and S. Diehl, *Rep. Prog. Phys.* **79**, 096001 (2016).
 [15] D. Leibfried, R. Blatt, C. Monroe, and D. Wineland, *Rev. Mod. Phys.* **75**, 281 (2003).
 [16] J. Koch, T. M. Yu, J. Gambetta, A. A. Houck, D. I. Schuster, J. Majer, A. Blais, M. H. Devoret, S. M. Girvin, and R. J. Schoelkopf, *Phys. Rev. A* **76**, 042319 (2007).
 [17] R. J. Schoelkopf and S. M. Girvin, *Nature (London)* **451**, 664 (2008).
 [18] M. Dykman, *Fluctuating Nonlinear Oscillators: From Nanomechanics to Quantum Superconducting Circuits* (Oxford University Press, New York, 2012).
 [19] J. F. Poyatos, J. I. Cirac, and P. Zoller, *Phys. Rev. Lett.* **77**, 4728 (1996).
 [20] C. J. Myatt, B. E. King, Q. A. Turchette, C. A. Sackett, D. Kielpinski, W. M. Itano, C. Monroe, and D. J. Wineland, *Nature (London)* **403**, 269 (2000).
 [21] K. Vahala, M. Herrmann, S. Knünz, V. Batteiger, G. Saathoff, T. Hänsch, and T. Udem, *Nat. Phys.* **5**, 682 (2009).
 [22] D. Kienzler, H.-Y. Lo, B. Keitch, L. de Clercq, F. Leupold, F. Lindenfesler, M. Marinelli, V. Negnevitsky, and J. Home, *Science* **347**, 53 (2015).
 [23] E. T. Holland, B. Vlastakis, R. W. Heeres, M. J. Reagor, U. Vool, Z. Leghtas, L. Frunzio, G. Kirchmair, M. H. Devoret, M. Mirrahimi, and R. J. Schoelkopf, *Phys. Rev. Lett.* **115**, 180501 (2015).
 [24] J. Roßnagel, S. T. Dawkins, K. N. Tolazzi, O. Abah, E. Lutz, F. Schmidt-Kaler, and K. Singer, *Science* **352**, 325 (2016).
 [25] M. Fitzpatrick, N. M. Sundaesan, A. C. Y. Li, J. Koch, and A. A. Houck, *Phys. Rev. X* **7**, 011016 (2017).
 [26] A. Mari, A. Farace, N. Didier, V. Giovannetti, and R. Fazio, *Phys. Rev. Lett.* **111**, 103605 (2013).
 [27] T. E. Lee and H. R. Sadeghpour, *Phys. Rev. Lett.* **111**, 234101 (2013).
 [28] T. E. Lee, C.-K. Chan, and S. Wang, *Phys. Rev. E* **89**, 022913 (2014).
 [29] S. Walter, A. Nunnenkamp, and C. Bruder, *Phys. Rev. Lett.* **112**, 094102 (2014).
 [30] S. Walter, A. Nunnenkamp, and C. Bruder, *Ann. Phys.* **527**, 131 (2015).
 [31] M. Xu, D. A. Tieri, E. C. Fine, J. K. Thompson, and M. J. Holland, *Phys. Rev. Lett.* **113**, 154101 (2014).
 [32] M. Xu and M. J. Holland, *Phys. Rev. Lett.* **114**, 103601 (2015).
 [33] V. Ameri, M. Eghbali-Arani, A. Mari, A. Farace, F. Kheirandish, V. Giovannetti, and R. Fazio, *Phys. Rev. A* **91**, 012301 (2015).
 [34] N. Lörch, E. Amitai, A. Nunnenkamp, and C. Bruder, *Phys. Rev. Lett.* **117**, 073601 (2016).
 [35] T. Weiss, S. Walter, and F. Marquardt, *Phys. Rev. A* **95**, 041802 (2017).
 [36] F. Galve, G. L. Giorgi, and R. Zambrini, arXiv:1610.05060.

- [37] G. L. Giorgi, F. Galve, and R. Zambrini, *Phys. Rev. A* **94**, 052121 (2016).
- [38] J. R. Johansson, G. Johansson, and F. Nori, *Phys. Rev. A* **90**, 053833 (2014).
- [39] L. E. de Clercq, H.-Y. Lo, M. Marinelli, D. Nadlinger, R. Oswald, V. Negnevitsky, D. Kienzler, B. Keitch, and J. P. Home, *Phys. Rev. Lett.* **116**, 080502 (2016).
- [40] S. Rips, M. Kiffner, I. Wilson-Rae, and M. J. Hartmann, *New J. Phys.* **14**, 023042 (2012).
- [41] Note that the dissipators in Eq. (2) have no off-diagonal elements between each other in the Lindblad equation [40]. Depending on the concrete system and parameters, these coherences may be present. The effects we want to show exist in both cases, though, so we use this simpler model here.
- [42] M. Grimm, C. Bruder, and N. Lörch, *J. Opt.* **18**, 094004 (2016).
- [43] R. Barak and Y. Ben-Aryeh, *J. Opt. B* **7**, 123 (2005).
- [44] M. R. Hush, W. Li, S. Genway, I. Lesanovsky, and A. D. Armour, *Phys. Rev. A* **91**, 061401 (2015).
- [45] C. Davis-Tilley and A. D. Armour, *Phys. Rev. A* **94**, 063819 (2016).
- [46] See Supplemental Material at <http://link.aps.org/supplemental/10.1103/PhysRevLett.118.243602> for an analytical model and further illustrations of the quantum synchronization blockade, a discussion of a network of four oscillators, and a discussion of the minimal model to show the effect.
- [47] A. J. Rimberg, M. P. Blencowe, A. D. Armour, and P. D. Nation, *New J. Phys.* **16**, 055008 (2014).
- [48] J. R. Souquet and A. A. Clerk, *Phys. Rev. A* **93**, 060301(R) (2016).
- [49] R. Ma, C. Owens, A. Houck, D. I. Schuster, and J. Simon, *Phys. Rev. A* **95**, 043811 (2017).
- [50] K. Brown, C. Ospelkaus, Y. Colombe, A. Wilson, D. Leibfried, and D. Wineland, *Nature (London)* **471**, 196 (2011).
- [51] M. Harlander, R. Lechner, M. Brownnutt, R. Blatt, and W. Hänsel, *Nature (London)* **471**, 200 (2011).
- [52] J. Johansson, P. Nation, and F. Nori, *Comput. Phys. Commun.* **184**, 1234 (2013).
- [53] J. Bezanson, A. Edelman, S. Karpinski, and V. B. Shah, *SIAM Rev.* **59**, 65 (2017).